Visualization Blackboard

Editors: Lloyd Treinish and Deborah Silver

Multilevel Visualization of Spinal Reflex Circuit Simulations

Kalpathi R. Subramanian, David P. Bashor, William V. Hasty, and Sandra M. Merkel

University of North Carolina at Charlotte

Few tools exist for the system-level investigation of nervous system function, just electroencephalography (EEG), functional brain imaging techniques, and large-scale simulation. Of these, simulation has contributed the least to our understanding. This is unfortunate, as simulation has much to offer:

- It provides a powerful way to synthesize experimental data into a coherent system whose dynamic behavior we can examine.
- Creating a simulation sets out a theory, contributing to the existing body of brain function theories.
- It can show us how system-level behavior emerges from lower-level (cellular, synaptic, and anatomical) properties.
- It can combine the temporal resolution of EEG techniques with the spatial resolution of functional brain imaging.
- Computing power and software tools are readily available.

Here we describe the construction and application of a simulation environment that uses visualization as the interface to control and analyze the behavior of spinal reflex circuits. This use of visualization as a primary output for simulation is somewhat unusual, and we find it very powerful. The environment facilitates rapid experimentation because it gives immediate visual feedback on the impact of a change in input, which can be followed by statistical analysis. Rapid feedback will sometimes permit further experimentation without a complete statistical analysis. The tool thus considerably speeds the development cycle of new experiments, as well as providing the usual benefits of data visualization.

Spinal reflexes represent some of the building blocks of motor control. To study the neuronal interactions producing these simple behaviors, Bashor[1] has built (from published algorithms[2]) a physiologically reasonable computational model of how the classical "stretch" and Golgi tendon organ reflexes operate to control pairs of opposing muscles at a single joint. We seek to understand how the dynamic interactions among neurons in the various populations produce observed behaviors of the output elements, the opposing motoneurons (populations #1 and #2 in Figure 1). The model's present form, shown in Figure 1, includes 15 cell populations (1,500 neurons) and seven fiber input populations (700 input elements). Individual neurons in the simulation are based on an "integrate and fire" algorithm, with state variables membrane potential (E), threshold potential (TH), potassium conductance (GK, the "recovery" variable), and spike occurrence (S). The neurons in all cell populations are driven by randomly occurring excitatory conductance charges; this input gives a background against which we can measure the effects of sensory inputs.

Basic design elements

An experiment typically represents 1.5 seconds of real time (at a resolution of 1 ms), of which we disregard the first 100 ms for network initialization. We divide the experiment into three time periods:

1. a control period (100-499 ms),
2. a stimulus period (500-749 ms), during which selected inputs are activated, and
3. a recovery period (750-1,500 ms), during which the network returns to (or toward) its control state.

We thus want the following data about the simulation: number of cells active in each population, frequency of action potential (spike) production by cells in each population, and basic statistics on the intervals between spikes for any desired time period. We are also interested in the relationship of activity in one population to that of populations both "upstream" and "downstream"; this was a major driving force in the visualization system's design.

Because of the simulation's size, an experiment generates a large amount of data, making processing laborious (up to 40 hours for a complete analysis). Even then, the statistical data, frequency histograms, and simple *X-Y* plots did not present much of the dynamic interaction occurring within and among populations. We thus designed an automated simulation system that included visualization of individual cell activity for all populations.

Visualization design

The visualization system we constructed performs the simulation and visualizes the circuit behavior as a function of time. A 1.5-second experiment (used to generate

May–June 1997

1 Spinal circuit showing interconnections among populations (assembled from the literature).

the illustrations here) takes about 90 seconds (this time is a function of the number of cells active and their rate of firing) on an SGI Indigo2 workstation. As the simulation progresses, the membrane and threshold potential values of all cells and the identity of the firing cells are recorded in a data structure (an array of lists, indexed by time step). We did this for two reasons. First, the simulation will not be a bottleneck in generating the visualizations. More important, it allows repeated review (forwards and backwards) of the simulation, implemented via a VCR-type interface as illustrated in Figure 2 (next page). On an SGI Indigo2 with Impact Graphics, the current system can display all 22 populations (with three state variables per cell population) at a rate of 10

time steps (or frames) per second (which is actually too fast for analysis purposes). We built the visualization system using SGI's Open Inventor toolkit with a Motif widget-based user interface. We chose Inventor because it provides high performance, greater implementation flexibility, and built-in features for viewing and interaction.

Single neurons being the basic elements of the simulation, we designed the visualization around them. We envisioned the 100 cells of each population as being laid out on a grid (implemented using quad meshes), although because of the wraparound algorithm for handling connections, mathematically they exist on a seamless torus. Three of the four state variables (*E*, *TH*, and *S*) for every neuron in the simulation are directly rep-

2 Visualization system interface.

resented. Each variable appears as a height field. Thus, as the function values change over the grid, the quad mesh vertices are proportionally scaled to reflect the changes in the function. The field values directly determine the amounts by which the membrane potential and threshold fields are raised (no additional scaling is performed), while the spike field is scaled by a user-defined value.

While not currently implemented, adding a vertical axis would help in comparing the voltage levels between populations. In the bottom left panel of Figure 2, we see three populations (300 cells), each represented by three height fields (gray, green, and yellow). The green field shows membrane potential (the excitability level of each cell), updated at each millisecond. Each cell's membrane potential varies with

- synaptic conductance changes (input) arriving at each time from other cells or fibers, and
- time since the last spike in that cell.

Thus, the level of the green field represents the probability of spike production.

The field's roughness represents cells' different states of readiness to produce a spike, that is, the amount of fragmentation in the population. Cells in the left and right populations in the figure are quite fragmented, while those in the middle population are at about the same potential level. The yellow field represents the threshold, that is, the readiness for spike production; when the membrane potential equals or exceeds the threshold potential, a spike is produced. The firing threshold depends on the time since that cell's last spike. When the green field touches or crosses the yellow field, we know a spike has occurred. However, spike occurrence being such an important event, we represent it separately in the gray (lowest) field to most rapidly convey this information.

In Figure 2, the left population is producing several spikes (green field penetrating yellow); the middle population, none (green and yellow fields far apart); and the right, two. The bottom right panel in Figure 2 shows activity in a fiber population (#22) and a cell population. Fiber populations have no membrane potential, only spike activity with some probability of occurrence. Fiber populations provide the inputs to the cell populations. The cell population is producing no spikes in the time frame shown.
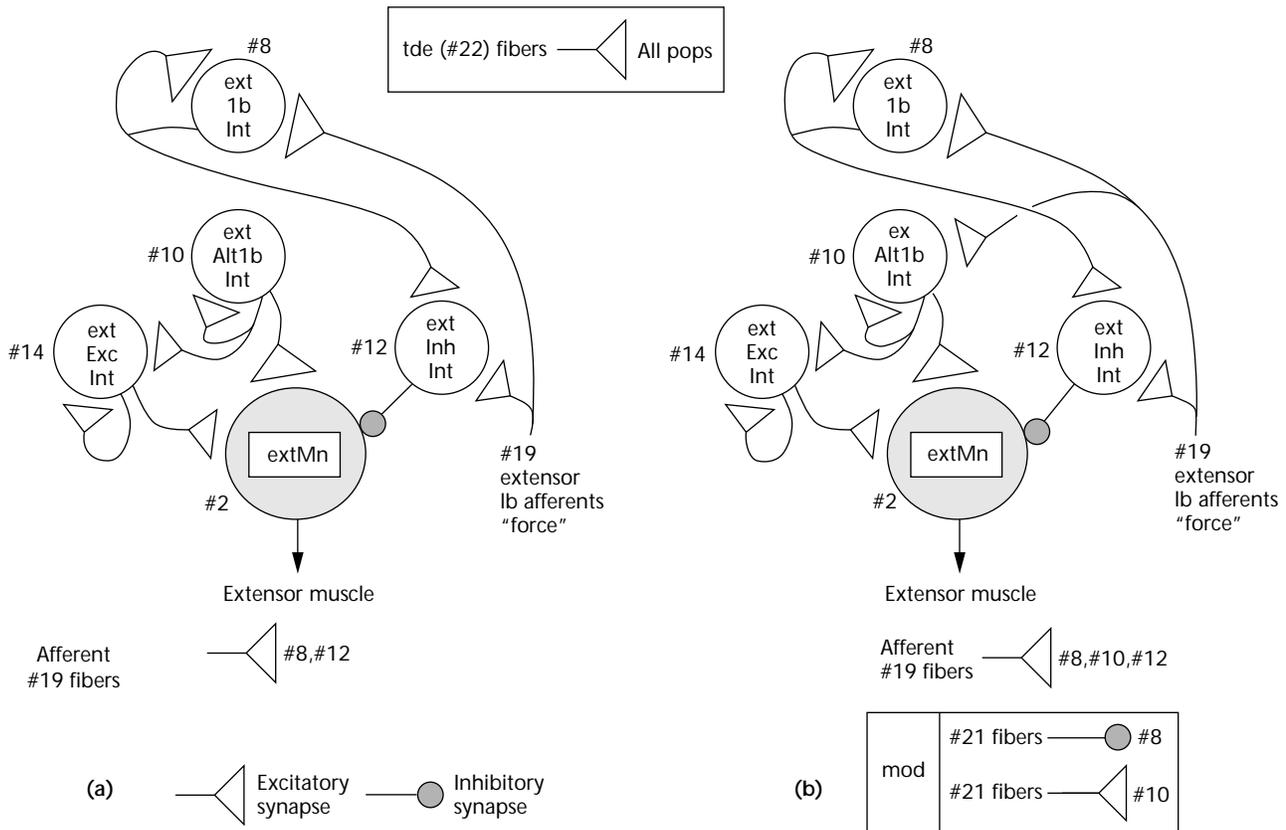
3 These two circuit diagrams for simulated normal and alternate Golgi tendon reflexes represent different experimental conditions. Some cells are active in all populations during the control period because of continuing random excitation through fiber population #22. (a) The "classic" Golgi tendon reflex. (b) A possible wiring pattern that changes the inhibitory effect into an excitatory one.

A representative experiment

Recent experimental studies have addressed how force-measuring sensory mechanisms influence spinal-level motor control. We have created some simulations (two of which are extracted here) to help clarify experimental issues and suggest mechanisms by which sensory input from the force-measuring elements of muscle (the Golgi tendon organs) may influence spinal circuits. A typical textbook view of force feedback shows an inhibitory circuit in which force production by a muscle (activity in fiber population #19) tends to reduce motoneuron (population #2) activity and hence force output.[3] Figure 3a (a subset of Figure 2) represents this hypothesis. During the stimulus period, when population #19 (Golgi tendon afferents) is active, populations #8 and #12 exhibit increased activity. This increase is reflected in lowered excitability of population #2, because #12 inhibits #2.

However, several studies suggest that Golgi tendon input to the nervous system can contribute to increased force output (motoneuron activity) during standing and walking. Figure 3b shows a hypothetical wiring diagram, consistent with the literature findings, that would produce this effect. In this circuit, population #19 excites not only #8 and #12 but also #10, the alternate Ib interneurons. The alternate Ib interneurons excite motoneuron firing, thus counteracting (and in this experiment overcoming) the inhibition produced

by the action of cells in populations #8 and #12. The balance between inhibition and excitation is determined by fiber population #21, which inhibits population #8 and excites #10.

Figure 4 (on the next page) is a very small illustration of the overall finding of these simulations. It shows one use of the visualization system and represents the same three consecutive frames from the stimulus period of the two experiments. The top row of images shows motoneuron activity decreasing under the influence of Ib interneuron (#8) and inhibitory interneuron (#12) activity. In other words, the Golgi tendon organ activity ultimately caused more motoneuron inhibition than excitation. Conditions in the second experiment (bottom row) resulted in the motoneurons (#2) receiving more excitation than inhibition. Even though the Ib interneuron (#8) activity appears to increase over this time, it is strongly counteracted by the increased activity in the alternate Ib (#10) and excitatory interneuron (#14) populations. This difference arose from two different kinds of changes, summarized in Figure 3b:

1. Golgi tendon organ activity (#19) excites alternate Ib interneurons (#10), which excite motoneurons directly and through excitatory interneurons (#14).
2. At the same time, the excitability of population #8 was lowered and #10 excitability was raised by activity in fiber population #21.

Summary

The new simulation environment gives us numerous important benefits as we investigate the interaction among large numbers of neurons in multiple populations. The visualizations let us easily see differences in excitability within and between populations as well as their changes over time. The smoothness of the potential height field visualizes the fragmentation of neuron activity within the population. These were not available before, and the visual form provides an excellent choice for assessing this property. The voltage height field differences between populations brought to our attention new aspects to which we needed to turn our quantitative tools. The system also tracks more variables than previously recorded, making more aspects of the simulation available for statistical analysis.

The system evolves continually as we use it and formulate new experimental questions. We plan conceptually simple changes like altering the number of neurons in a population and adding populations. These should involve minimal effort and make the system more amenable to simulating larger models, such as those controlling more muscles at multiple joints. Visually representing the transmission of activity among populations is another important component missing from the current system. Also, while height fields are a simple and straightforward representation of the activity in each population, we need to explore alternate representations, perhaps a toroidal representation of the neuron populations with color-coded connections (more representative of the actual connection algorithm used), or something as simple as color-coded images. One advantage of using height fields is the ease of observing the amount of activity in each population.

In its current form, the simulation environment provides a movie of neuronal activity within the various populations (for a sample movie, see http://www.cs.uncc.edu/~krs/publ.html). The statistical analysis of the generated data could also benefit from multivariate visualization techniques, in contrast to simple 2D plots that just relate individual cell or population measures. Such an approach opens possibilities for visualizing the statistical measures of multiple cells or populations, suitably distinguished from each other. Finally, tools to measure quantitative information to compare populations (one variable at a time, for instance) or track individual neurons would prove useful in the analysis step. ∎

References

1. D.P. Bashor, "A Model of Some Reflex Components of the Spinal Motor System," submitted to *Biological Cybernetics*.
2. R.J. MacGregor, *Neural and Brain Modeling*, Academic Press, New York, 1987.
3. D.P. Bashor and S.M. Merkel, "Simulation of Spinal Segmental Reflexes: The Alternate Golgi Reflex," *Soc. for Neuroscience Abstracts*, Vol. 22, No. 2, 1996, p. 1372.

Readers interested in this research may contact Subramanian at the Department of Computer Science, University of North Carolina at Charlotte, Charlotte, NC 28223, e-mail krs@mail.cs.uncc.edu.

To submit a column to Visualization Blackboard, contact editors Lloyd Treinish (e-mail lloydt@watson.ibm.com) or Deborah Silver (e-mail silver@vizlab.rutgers.edu).
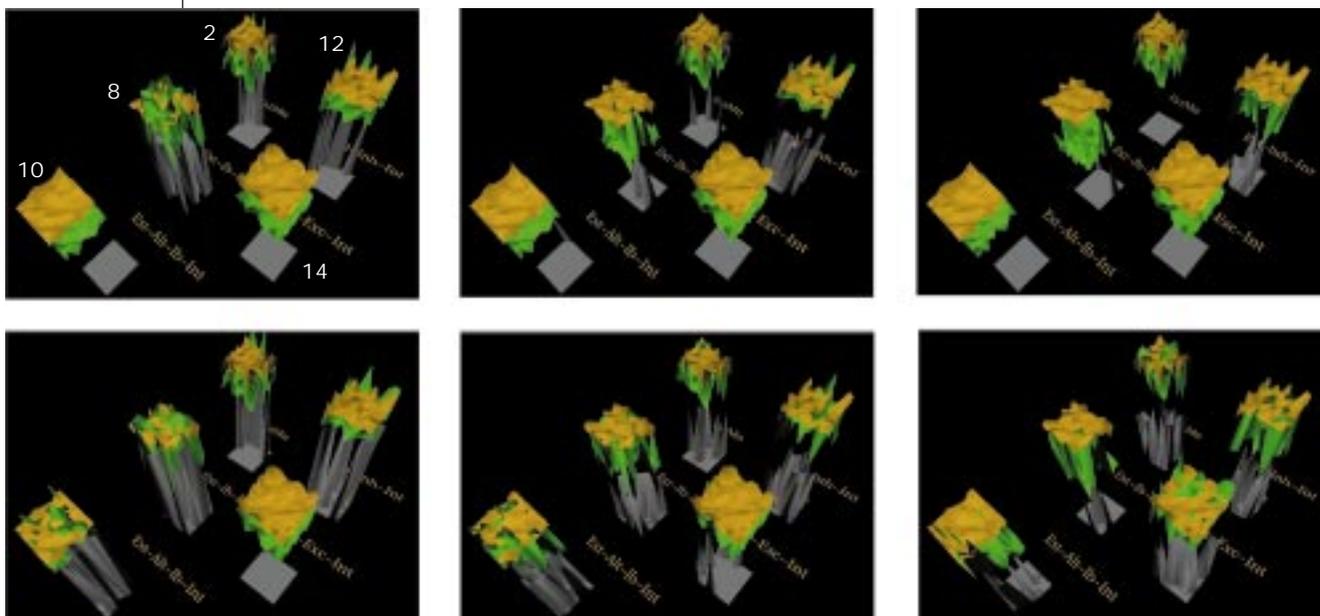
4 Golgi tendon reflexes. Top row: A 3-ms sequence for the conditions of Figure 3a. Motoneuron (#2) activity decreases under the influence of Ib (#8) and inhibitory (#12) interneuron activity. Only one spike appears in the alternate Ib interneurons (#10), and no spikes appear in the excitatory interneurons (#14). Bottom row: The same 3-ms sequence for the conditions of Figure 3b. Over this time period, motoneuron (#2) activity increases rather than decreases.